NAVAL POSTGRADUATE SCHOOL

MONTEREY, CALIFORNIA

THESIS

THE EFFECTS OF EARTH'S ROTATION ON THE LATE SUBMARINE WAKE

by

David J. Lorfeld

December 2017

Thesis Advisor: Timour Radko
Co-Advisor: John Joseph

Approved for public release. Distribution is unlimited.

THIS PAGE INTENTIONALLY LEFT BLANK

REPORT DOCUMENTATION PAGE			Form Approved OMB No. 0704-0188

1. AGENCY USE ONLY *(Leave blank)*	2. REPORT DATE December 2017	3. REPORT TYPE AND DATES COVERED Master's thesis

4. TITLE AND SUBTITLE THE EFFECTS OF EARTH'S ROTATION ON THE LATE SUBMARINE WAKE	5. FUNDING NUMBERS
6. AUTHOR(S) David J. Lorfeld	
7. PERFORMING ORGANIZATION NAME(S) AND ADDRESS(ES) Naval Postgraduate School Monterey, CA 93943-5000	8. PERFORMING ORGANIZATION REPORT NUMBER
9. SPONSORING /MONITORING AGENCY NAME(S) AND ADDRESS(ES) N/A	10. SPONSORING / MONITORING AGENCY REPORT NUMBER

11. SUPPLEMENTARY NOTES The views expressed in this thesis are those of the author and do not reflect the official policy or position of the Department of Defense or the U.S. Government. IRB number ____N/A____.

12a. DISTRIBUTION / AVAILABILITY STATEMENT Approved for public release. Distribution is unlimited.	12b. DISTRIBUTION CODE

13. ABSTRACT (maximum 200 words)

Detection and tracking of submarines by acoustic means alone has become increasingly difficult due to quieter submarines, which underscores the need for non-acoustic detection methods. One hydrodynamic method available is through wake detection and the tracking of the resulting vortices created by the turbulence. Until now, it has been assumed that these vortices have large enough Rossby numbers such that the rotation of the Earth can be ignored. This study examines the vortices that persist in the late submarine wake and explores the effects of rotation on the detectable characteristics of these wakes. Numerical simulations were used to model the vortices in the late submarine wake with and without rotation. Comparisons between these results have shown that the direction of rotation of vortices in the late submarine wake are affected by the rotation of the Earth and that Coriolis force must be taken into account.

14. SUBJECT TERMS pancake vortices, stratified wake, late wake, rotation, Coriolis force, cyclonic and anticyclonic vorticity	15. NUMBER OF PAGES 45
	16. PRICE CODE

17. SECURITY CLASSIFICATION OF REPORT	18. SECURITY CLASSIFICATION OF THIS PAGE	19. SECURITY CLASSIFICATION OF ABSTRACT	20. LIMITATION OF ABSTRACT
Unclassified	Unclassified	Unclassified	UU

NSN 7540-01-280-5500 Standard Form 298 (Rev. 2-89) Prescribed by ANSI Std. 239-18

THIS PAGE INTENTIONALLY LEFT BLANK

Approved for public release. Distribution is unlimited.

THE EFFECTS OF EARTH'S ROTATION ON THE LATE SUBMARINE WAKE

David J. Lorfeld
Lieutenant Commander, United States Navy
M.S., The University of Southern Mississippi, 2013

Submitted in partial fulfillment of the
requirements for the degree of

**MASTER OF SCIENCE IN METEOROLOGY
AND PHYSICAL OCEANOGRAPHY**

from the

**NAVAL POSTGRADUATE SCHOOL
December 2017**

Approved by: Timour Radko
Thesis Advisor

John Joseph
Co-Advisor

Peter Chu
Chair, Department of Oceanography

THIS PAGE INTENTIONALLY LEFT BLANK

ABSTRACT

Detection and tracking of submarines by acoustic means alone has become increasingly difficult due to quieter submarines, which underscores the need for non-acoustic detection methods. One hydrodynamic method available is through wake detection and the tracking of the resulting vortices created by the turbulence. Until now, it has been assumed that these vortices have large enough Rossby numbers such that the rotation of the Earth can be ignored. This study examines the vortices that persist in the late submarine wake and explores the effects of rotation on the detectable characteristics of these wakes. Numerical simulations were used to model the vortices in the late submarine wake with and without rotation. Comparisons between these results have shown that the direction of rotation of vortices in the late submarine wake are affected by the rotation of the Earth and that Coriolis force must be taken into account.

THIS PAGE INTENTIONALLY LEFT BLANK

TABLE OF CONTENTS

THIS PAGE INTENTIONALLY LEFT BLANK

LIST OF FIGURES

THIS PAGE INTENTIONALLY LEFT BLANK

LIST OF TABLES

THIS PAGE INTENTIONALLY LEFT BLANK

LIST OF ACRONYMS AND ABBREVIATIONS

CF	Coriolis force
f	Coriolis parameter (1×10^{-4})
MITgcm	Massachusetts Institute of Technology General Circulation Model
MOW	Modified Okubo-Weiss
OW	Okubo-Weiss parameter
PGF	pressure gradient force
T_{BOT}	temperature at bottom of temperature gradient

THIS PAGE INTENTIONALLY LEFT BLANK

ACKNOWLEDGMENTS

Though a singular piece of work, this thesis is the result of efforts and contributions of numerous individuals. My deepest gratitude goes to my thesis advisor, Dr. Timour Radko. His excitement and passion for oceanography and fluid dynamics sparked an interest in an area I knew little about before our initial meeting. His guidance, and at times patience, were crucial to my success.

I would also like to thank my second reader, Mr. John Joseph. By steering me toward modeling work, he introduced me to a side of oceanography I had never before encountered. His practical knowledge and real-world experience were beneficial to not only this project, but to numerous other courses as well.

I cannot thank Dr. Justin Brown and Dr. Ryan Moll enough. They provided countless hours of assistance in every facet. Whether troubleshooting model runs, helping in the development of new code, or editing my work that was “just plain wrong,” their help is greatly appreciated. Without them, I would still be trying to find the command prompt.

Last, I would like to thank my family. My fiancée, Abby, was always able to keep me sane and focused throughout this process, while at the same time she has learned more about modeling than she ever wanted to. I have always had my parents’ full support, and this time was no different. Even though my mother is still waiting for me to become an engineer. Finally, my sisters, Paula and Karen. Whenever I struggled, they were always willing to listen and help me out. Then promptly reminded me that a second master’s degree still doesn’t make me a lawyer or doctor like them.

THIS PAGE INTENTIONALLY LEFT BLANK

I. INTRODUCTION

A. BACKGROUND

It is common knowledge that vortex structures are created in stratified fluids in the wake of an object as it passes. One such structure is a pancake vortex, so-called because of its flattened and elongated shape as a result of the effects of buoyancy. Though they are commonly found in stratified turbulent fluids, little is known of their development, structure, and decay (Sutyrin and Radko 2017). Pancake vortices develop on long timescales, relative to the initial passage of the object, but their properties can depend on the earlier stages of the wake.

Stratified wakes are defined by three distinct stages. The near wake (e.g., Radko 2001), or first stage, is defined by high velocities and active turbulent mixing. The intermediate wake (e.g., Moody et al. 2017), or second stage, has reduced vertical velocities due to buoyancy forces and the horizontal extents increase. This elongation in the horizontal plane and reduction in the vertical is where pancake vortices first begin to take shape. The final stage, the late wake, is controlled by vertical diffusion (Meunier and Spedding 2004).

The generation of pancake vortices was identified by Schooley and Stewart (1963) while studying wakes in stratified fluids. At this time, the vortices were observed as a feature that occurred between wake generation and wake collapse and the association between the vortices' structure and the buoyancy frequency was established; however, study of the vortices themselves was limited to aspects concerning wake development. Research into wake collapse continued (van de Watering et al. 1969; Lin and Pao 1979) and pancake vortices continued to be observed, yet there remained little emphasis on them outside of wake evolution. This trend continued and the lack of directed research of pancake vortices in the late wake was acknowledged by Spedding (1997); however, his focus was primarily on vortex formation and did not take into account the rotation of the earth. Long-lived vortices were observed during these laboratory experiments, however both the vortices and wakes remained fairly symmetric. In spite of this, Spedding

acknowledged that wakes and vortices in the ocean experience forcing not present in the laboratory and that real-world results may differ from the ones he achieved. Follow-up research conducted by Beckers et al. (2001) addressed the dynamics of pancake vortices, but again, did not take the earth's rotation into account in regards to the vortices' direction of rotation or symmetry of the wake.

The key features of the wake are determined by the following parameters. The buoyancy frequency, also known as the Brunt-Väisälä frequency, measures the significance of the density gradient in stratified wakes and is responsible for the creation of pancake vortices. It is a characteristic frequency of gravity waves, i.e., oscillatory motion in a fluid caused by gravity. The Brunt-Väisälä frequency is given by

$$\text{Brunt-Väisälä frequency} \qquad N^2 = -g\alpha \frac{\partial T}{\partial Z}, \tag{1}$$

which is defined in terms of the gravitational acceleration (g), the coefficient of thermal expansion (α), and the temperature gradient ($\frac{\partial T}{\partial Z}$). Though the Brunt-Väisälä frequency is typically defined by the density gradient, the effects of salt stratification have been ignored for this experiment. In a stable environment ($N^2 > 0$), a perturbed particle will return to its pre-disturbed location whereas in an unstable environment ($N^2 < 0$), a perturbed particle will not return.

Also of importance to stratified fluids is the Froude number. The Froude number describes the relative effects of inertia and external forcing (e.g., gravity) and is given by the following equation, where U is the velocity and H is the height or diameter of a submerged object:

$$\text{Froude number} \qquad Fr = \frac{U}{HN} \ . \tag{2}$$

One way to examine the effects of rotation on a stratified wake is the Rossby number. The Rossby number (Ro) is the ratio of velocity (U) to Coriolis force (f) and the associated length scale (L) and is given by

Rossby Number $$Ro = \frac{U}{fL} \ . \quad (3)$$

For large Rossby numbers, which are typical of pancake vortices (Ro ~ 20), it is assumed that Coriolis force and Earth's rotation do not affect vortices of the late wake (Riley and Lelong 2000) due to their perceived limited life span and small size. However, these vortices have been shown to serve as an indicator of an object's passage through the water column (Spedding 2014). Given that pancake vortices have been found to persist in the late wake for several days, the assumption that they are not affected by rotation has recently been challenged by Sutyrin and Radko (2017).

B. MOTIVATION

By recognizing and identifying pancake vortices, it is possible to non-acoustically detect and track submerged objects. Hydrodynamic methods of detection and tracking have grown in importance due to the reduced acoustic signature of modern submarines and unmanned underwater vehicles (UUV) that make them much harder to detect by traditional acoustic means. Given this need, the importance of accurately identifying wakes and pancake vortices has increased, and with it, the motivation for explaining and predicting their key physical properties. Among those properties, one of the most controversial is the issue of whether or not they are affected by Coriolis force.

Recent work has shown that Earth's rotation does affect pancake vortices and their life cycle; however, the dynamics and magnitude of this phenomenon is not yet fully understood (Sutyrin and Radko 2017). In order to further this area of research and address the effects of rotation, numerical simulations were utilized. Unlike real-world experiments, numerical simulations offer a cost-effective approach for study in a field which would otherwise be prohibitively expensive. By determining the extent of the effect of Coriolis force on pancake vortices, a better understanding of the late submarine wake will be gained and possibly enhance target location and tracking procedures.

THIS PAGE INTENTIONALLY LEFT BLANK

II. METHODOLOGY

A. NUMERICAL SIMULATIONS

The Massachusetts Institute of Technology General Circulation Model (MITgcm) was utilized to conduct all numerical simulations in this study. MITgcm is a finite-volume numerical model designed to study the circulation of both the atmosphere and ocean environments and has a non-hydrostatic capability. This is achieved through the use of the Navier-Stokes equations as the model's governing equations. This results in the model's ability to study both large- and small-scale phenomena (Marshall et al. 1997). The model is highly flexible and thus we were able to adapt it to our needs, making MITgcm an ideal choice based on the study's objectives.

In order to run MITgcm, two supercomputers were employed. The Department of Defense (DOD) Shared Resource Center's High Performance Computing Modernization Program Cray XE6m (Copper) and Stampede2, of The University of Texas at Austin's Texas Advanced Computing Center were primarily employed to run the model, generate outputs, and store results until transferred to and analyzed with local Naval Postgraduate School (NPS) computing

B. MODEL CONFIGURATION

Multiple model configurations were employed throughout the course of the research. The results reported herein are based on the computational domain extending for 1024 meters in the x and y-directions and 44 meters in the z-direction. The horizontal resolution was 2 meters, and the vertical resolution was 1 meter. Boundaries, or walls, were imposed on the sides of the box during initial runs but were later replaced by periodic boundary conditions in order to better simulate an unconfined, open ocean environment.

In order to represent a wake generated by a submerged propagating object in a simple and computationally effective manner a jet was introduced mid-level at a depth of 22 m and located at y = 512 m and flowed from left to right in the positive x direction. The initial state was geostrophically balanced. This balance was achieved by introducing

the initial density perturbation, designed to produce the pressure gradient force counteracting the Coriolis force associated with the jet's velocity. The jet's initial height and width were 10 m and 25 m, respectively. The jet's velocity, *U*, was varied for each Rossby number, while the cross-flow pattern was Gaussian in all experiments. The schematic of the model configuration is shown in Figure 1.

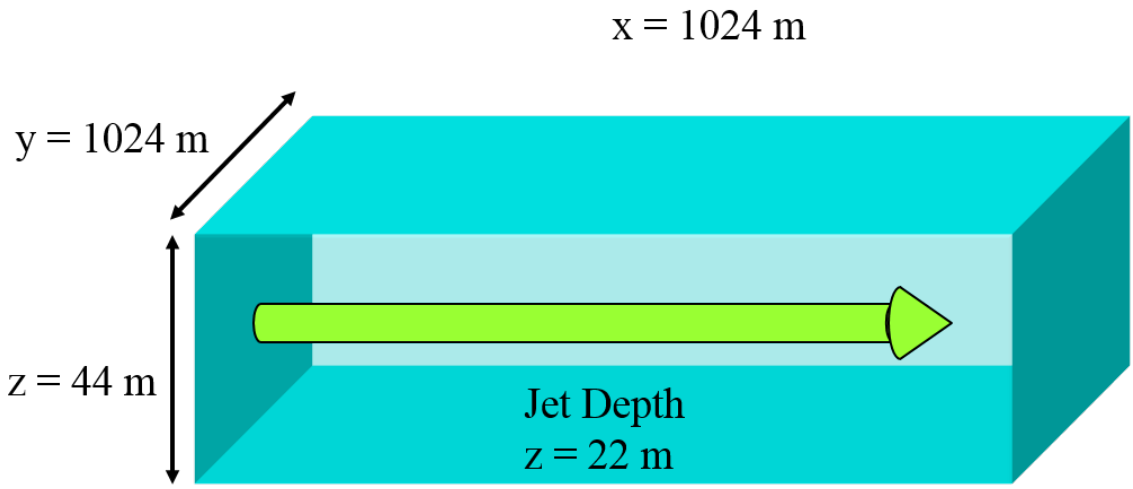

Figure 1. Model configuration and dimensions (not to scale)

For each series of model runs, either with Coriolis (f = 1 x 10^{-4} s^{-1}) or without (f = 0 s^{-1}), the jet velocity was determined by solving (Equation 3) for a given Rossby number. The jet velocity was then used to solve (Equation 2) for the Brunt-Väisälä frequency, *N*, and applied to each specific Froude number. The temperature gradient, $\frac{\partial T}{\partial Z}$, was calculated by solving the Brunt-Väisälä frequency equation (Equation 1) with a surface temperature of 20° C. These values are shown in Tables 1 (with Coriolis) and 2 (without Coriolis). The average value of 1 x 10^{-4} s^{-1} was chosen as a representative value of Coriolis force based on the mid latitudes.

Table 1. Input parameters for model runs with rotation

With Coriolis (f = 1 x 10^{-4} s^{-1})			
	Fr = 5	Fr = 15	Fr = 50
Ro = 20	U = 0.05 m/s N = 0.001 T_{BOT} = 19.9776	U = 0.05 m/s N = 3.33 x 10^{-4} T_{BOT} = 19.9975	U = 0.05 m/s N = 1 x 10^{-4} T_{BOT} = 19.9998
Ro = 50	U = 0.125 m/s N = 0.0025 T_{BOT} = 19.8597	U = 0.125 m/s N = 8.3 x 10^{-4} T_{BOT} = 19.9845	U = 0.125 m/s N = 2.5 x 10^{-4} T_{BOT} = 19.9986
Ro = 200	U= 0.5 m/s N = 0.01 T_{BOT} = 17.7551	U= 0.5 m/s N = 0.003 T_{BOT} = 19.7555	U= 0.5 m/s N = 0.001 T_{BOT} = 19.9776
Ro = 400	U = 1.0 m/s N = 0.02 T_{BOT} = 11.0204	U = 1.0 m/s N = 6.67 x 10^{-3} T_{BOT} = 19.0023	U = 1.0 m/s N = 0.002 T_{BOT} = 19.9102

Table 2. Input parameters for model runs without rotation

Without Coriolis (f = 0 s^{-1})			
	Fr = 5	Fr = 15	Fr = 50
U = 0.05 m/s	U = 0.05 m/s N = 0.001 T_{BOT} = 19.9776	U = 0.05 m/s N = 3.33 x 10^{-4} T_{BOT} = 19.9975	U = 0.05 m/s N = 1 x 10^{-4} T_{BOT} = 19.9998
U = 0.125 m/s	U = 0.125 m/s N = 0.0025 T_{BOT} = 19.8597	U = 0.125 m/s N = 8.3 x 10^{-4} T_{BOT} = 19.9845	U = 0.125 m/s N = 2.5 x 10^{-4} T_{BOT} = 19.9986
U= 0.5 m/s	U= 0.5 m/s N = 0.01 T_{BOT} = 17.7551	U= 0.5 m/s N = 0.003 T_{BOT} = 19.7555	U= 0.5 m/s N = 0.001 T_{BOT} = 19.9776
U = 1.0 m/s	U = 1.0 m/s N = 0.02 T_{BOT} = 11.0204	U = 1.0 m/s N = 6.67 x 10^{-3} T_{BOT} = 19.0023	U = 1.0 m/s N = 0.002 T_{BOT} = 19.9102

C. MODEL RUNS AND DIAGNOSTICS

A total of 24 simulations were completed utilizing MITgcm. Model runs with Coriolis force of f = 1 x 10^{-4} s^{-1} and with Rossby numbers of 20, 50, 200 and 400 were conducted, each with accompanying Froude numbers of 5, 15 and 50 for 12 runs. An

additional 12 runs with the same parameters were conducted with Coriolis force set equal to 0 s^{-1}. See Tables 1 and 2 for the parameters of each model run. To satisfy the Courant-Friedrichs-Lewy (CFL) condition, the time step was set to 0.05 s. In order to obtain the desired 66 model hours of data, each simulation required 24,576 core hours on a supercomputer. Upon completion of the 96-hour model run, salinity, temperature and velocity (both U and V components) output data were downloaded, analyzed, and plotted. Typical outputs of salinity and vorticity fields are shown in Figures 2 and 3.

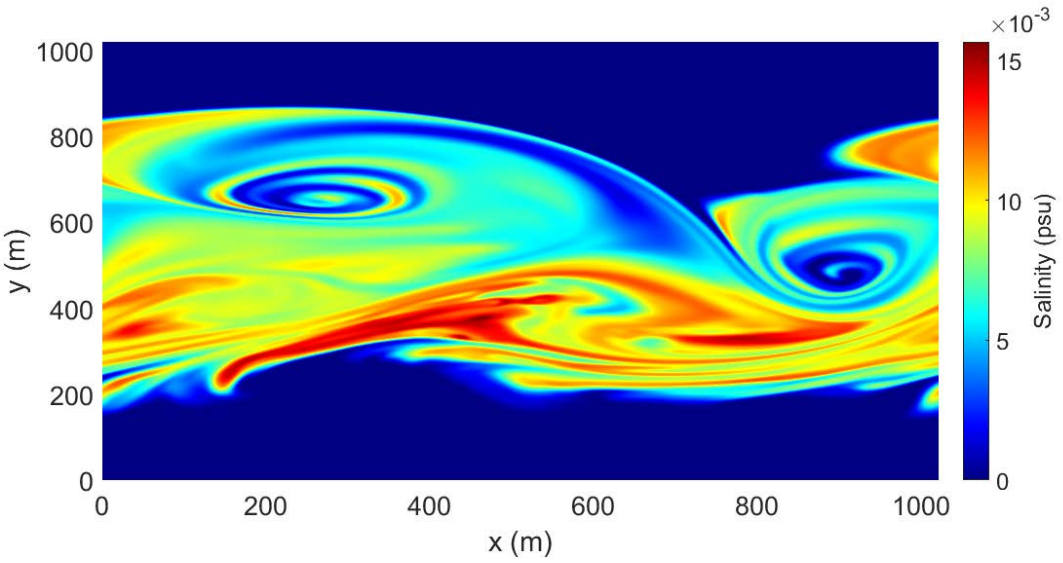

Tracer cross section for f = 1x10^{-4} s^{-1}, Ro = 50, Fr = 50 at a depth of 22 m at time 66.67 hours.

Figure 2. Tracer cross section

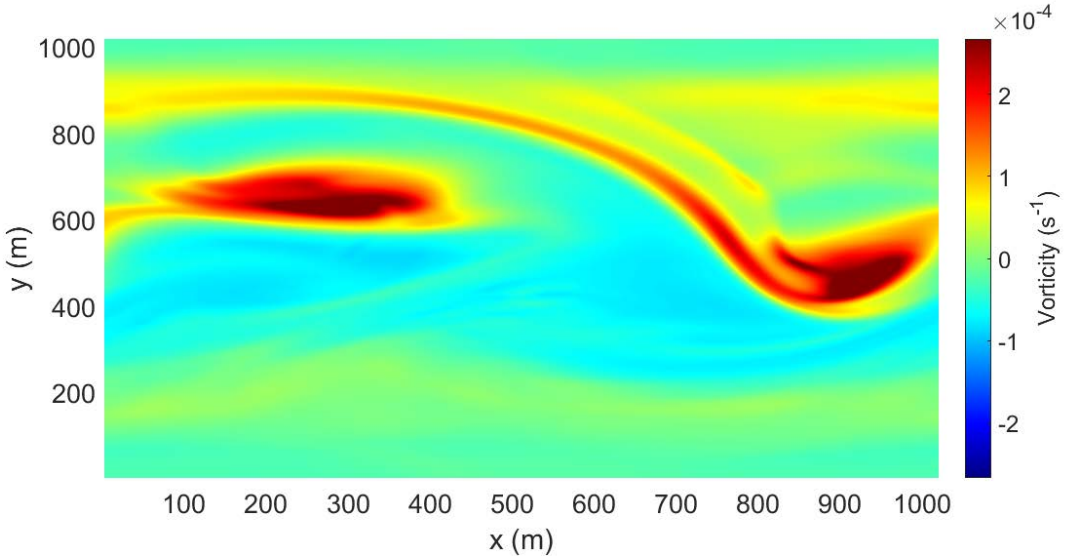

Vorticity cross section for f = 1x10^{-4} s^{-1}, Ro = 50, Fr = 50 at a depth of 22 m at time 66.67 hours.

Figure 3. Vorticity cross section

Figures 2 and 3 are the typical horizontal cross sections at a depth of 22 meters of the tracer and vorticity fields for a simulation with rotation. The neutrally buoyant tracer was initially placed along the jet and then passively advected by the velocity field. For this simulation, the Rossby number and Froude number are both 50. In Figure 2, the coherent structure of the wake remains evident more than 66 hours after the initiation of the experiment. Figure 3 displays the vorticity, with warm colors indicating positive (cyclonic) vorticity and cool colors indicating zero or negative (anti-cyclonic) vorticity.

In order to identify pancake vortices in model run results, an Eulerian vice Lagrangian approach was taken. A Lagrangian approach focuses primarily on an individual particle moving through a fluid whereas an Eulerian method focuses on various properties of the velocity field at a given location. Three specific Eulerian properties utilized for this study include velocity, vorticity, and the Okubo-Weiss parameter (OW).

The Okubo-Weiss parameter determines whether an area is either strain-dominated or vorticity-dominated. A positive OW reflects a strain-dominated area

whereas a negative OW reflects an area dominated by vorticity. The negative OW values were utilized as these values represent the presence of vortices in the modeled flow field. The Okubo-Weiss parameter and associated components are given by the following equations as presented by Vortmeyer-Kley et al. (2016):

Okubo-Weiss parameter $$OW = s_n^2 + s_s^2 - \omega^2 \tag{4}$$

Normal strain $$s_n = \frac{\partial u}{\partial x} - \frac{\partial v}{\partial y} \tag{5}$$

Shear strain $$s_s = \frac{\partial v}{\partial x} + \frac{\partial u}{\partial y} \tag{6}$$

Relative vorticity $$\omega = \frac{\partial v}{\partial x} - \frac{\partial u}{\partial y} \tag{7}$$

The Okubo-Weiss parameter was especially helpful in identifying and tracking pancake vortices; however, OW does not provide the direction of rotation of the vortex. In order to quantify the rotational direction and magnitude of the pancake vortices, OW was modified as follows. For each instance of time of the model run, the value of OW was calculated. For a negative OW (vortices present), the absolute value of OW was multiplied by the vorticity that was calculated for the same time interval. The resulting modified Okubo-Weiss value (MOW) allowed for objective identification of the vortices present at each time step along with their cyclonic or anticyclonic direction of rotation. The modified Okubo-Weiss is defined in Equation 8 as

$$MOW = \begin{cases} |OW| \cdot \omega < 0 = \text{anticyclonic rotation} \\ |OW| \cdot \omega > 0 = \text{cyclonic rotation} \end{cases} \quad for \quad OW < 0. \tag{8}$$

Calculated MOW values corresponding to the vorticity field found in Figure 3 are shown in Figure 4.

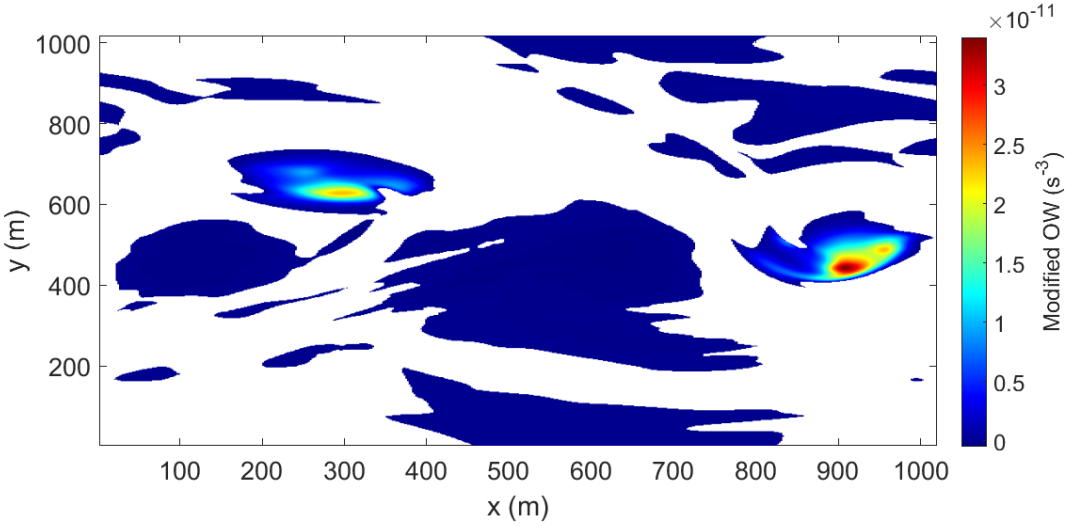

MOW cross section for f = 1x10^{-4} s^{-1}, Ro = 50, Fr = 50 at depth 22 m and time 66.67 hours. The white regions are strain-dominated where MOW is not calculated.

Figure 4. MOW cross section

In order to determine whether a given flow regime is dominated by cyclonic or anticyclonic vortices, we also introduced an integral measure of the rotational preference (A) as follows. The spatial average of the MOW value at a given time was divided by the corresponding spatial average of the absolute value of the MOW, as shown in Equation 9

$$A = \frac{\overline{(MOW)}_{xyz}}{(|MOW|)_{xyz}}. \tag{9}$$

If the resulting value, A, was positive, the field at that time step was cyclone-dominated. For negative values of A, anticyclones dominated the field. The greater the value trended towards 1.0 (-1.0), the greater the relative intensity of cyclonic to anticyclonic (anticyclonic to cyclonic) vortices. A near zero A represented a parity of rotation, where cyclonic and anticyclonic vortices existed in near equal amounts.

THIS PAGE INTENTIONALLY LEFT BLANK

III. RESULTS

This study focused on the potential effects of rotation and the associated impacts on pancake vortices. Presented in Section A are the results from runs with rotation and are followed (Section B) by the results without rotation. A comparison between the two data sets is then presented.

A. WITH CORIOLIS

Model runs conducted with rotation experienced both cyclonic and anticyclonic vortices in the early stages following the destabilization of the jet. These vortices were evident in all Rossby and Froude number combinations. At Ro=20, the vortices became loosely defined and structured, but for simulations with larger Rossby numbers, the vortices were more structured and coherent. This is believed to be a result of the increase in jet velocity accompanying the higher Rossby number and the associated increase in turbulence that the greater speeds induced. Figures 5–8 are vorticity plots for each Rossby number at time 66.67 hours and show the vortices' structure. Positive values reflect cyclonic rotation and negative values reflect anticyclonic rotation.

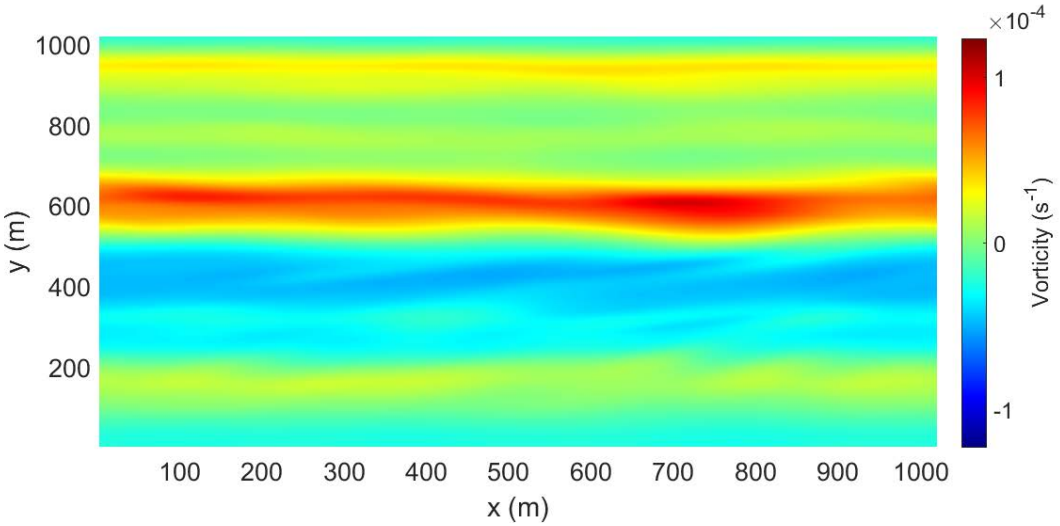

Figure 5. Vorticity cross section, Ro = 20, Fr = 5

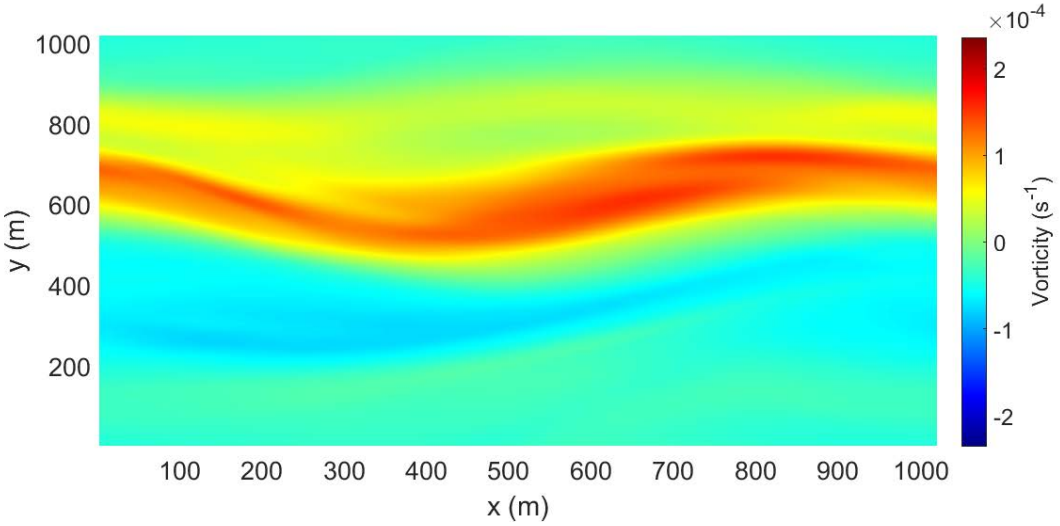

Figure 6. Vorticity cross section, Ro = 50, Fr = 5

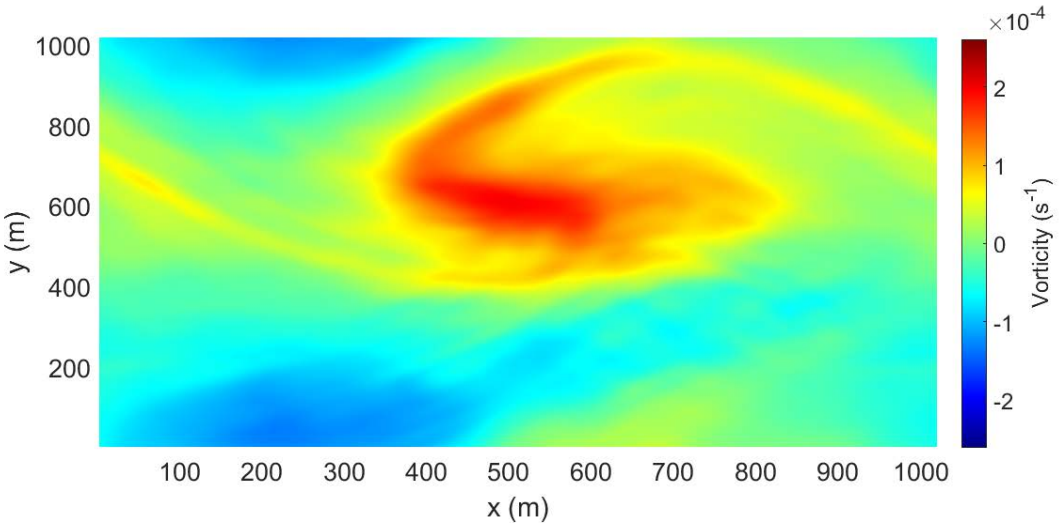

Figure 7. Vorticity cross section, Ro = 200, Fr = 5

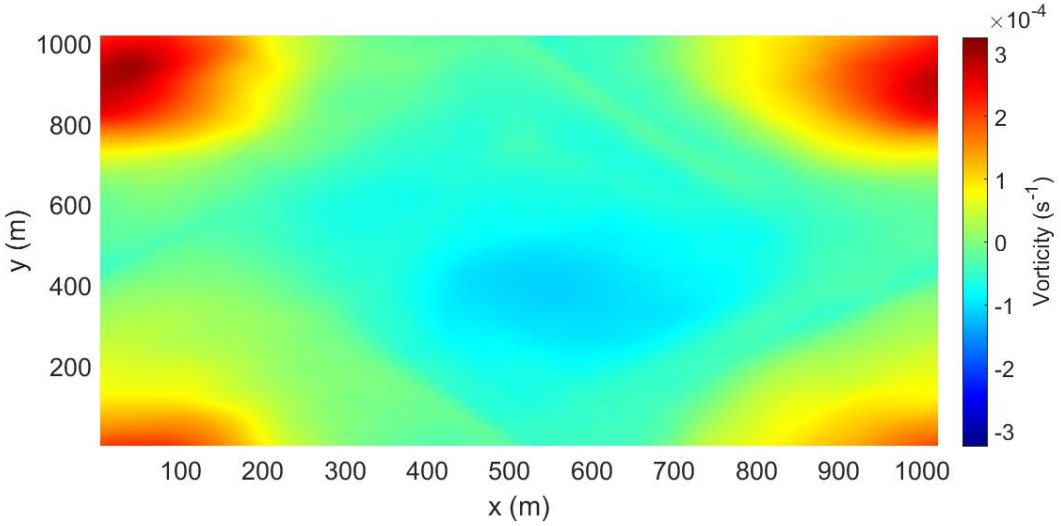

Figure 8. Vorticity cross section, Ro = 400, Fr =5

As each model run progressed in time, the anticyclonic vortices diminished in size, and their numbers decreased while the cyclonic vortices persisted and grew. The disparity between the number of cyclonic and anticyclonic vortices was evident in all Rossby and Froude number combinations but was much more prevalent at the higher Rossby numbers. For a given Rossby number, the largest difference between the sign of the vortices occurred at the highest Froude number. As a result of the difference in the number of cyclonic and anticyclonic vortices, an asymmetric wake pattern developed. The dominance of cyclonic vortices is attributed to the disintegration of anticyclones by centrifugal instability, as suggested by Sutyrin and Radko (2017).

B. WITHOUT CORIOLIS

Model runs conducted without the Coriolis force experienced both cyclonic and anticyclonic vortices. Both types of vortices persisted throughout the entire duration of the runs. Though continuously present, the structure and the coherence of the vortices varied among the model runs. Vortices were generally more organized and coherent at the lower velocity runs than the higher velocity runs. Figures 9 and 10 show the difference in structure between velocities of 0.125 m/s and 1.0 m/s at the same Froude

number and time period. Though the vortices were less coherent at higher jet velocities, both cyclonic and anticyclonic rotation remained.

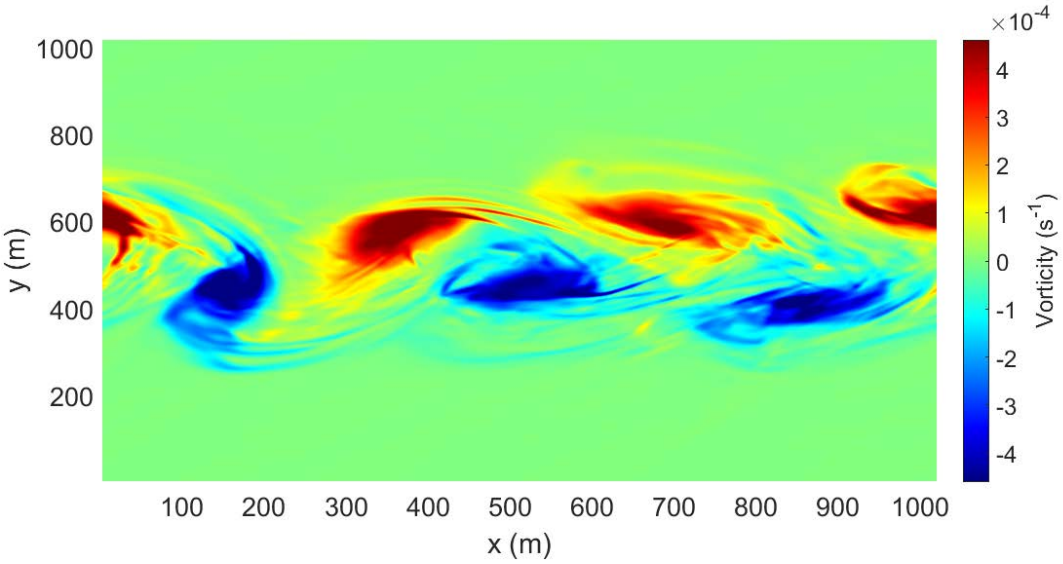

Figure 9. Vorticity cross section, U = 0.125 m/s, Fr = 5

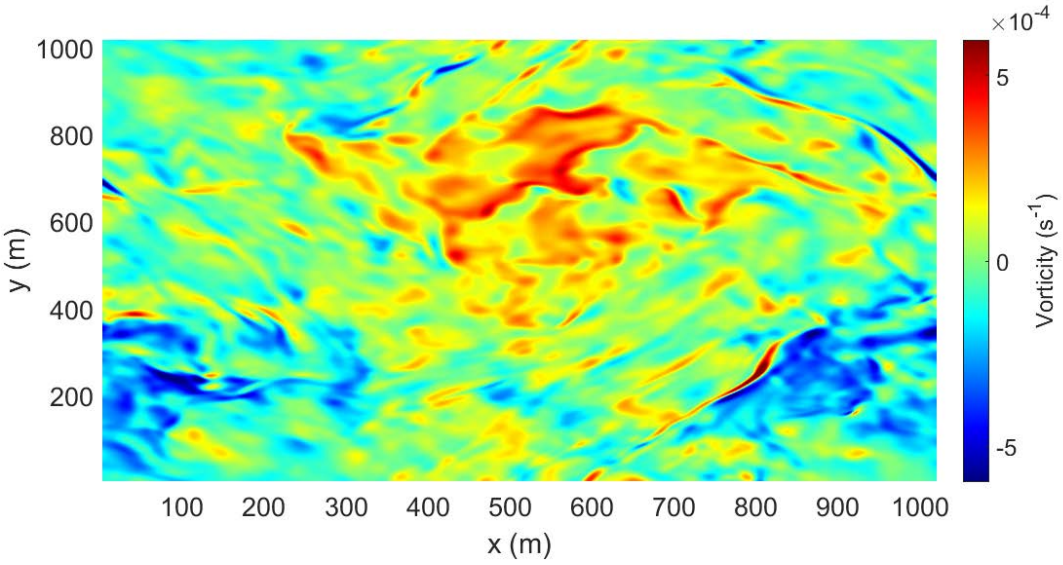

Figure 10. Vorticity cross section, U = 1.0 m/s, Fr = 5

C. COMPARISON OF RESULTS

As previously mentioned in Chapter II, Section B, the only parameter that was changed between the two sets of model runs was the inclusion or exclusion of planetary rotation. For those runs without rotation, it is clear to see that both cyclonic and anticyclonic vortices persist throughout the entire period. For the runs in which rotation was included, this is not the case. Though both directions of vortices were present in the early stages of each model run, the number and size of anticyclonic vortices in the simulations with rotation decreased over time. This result is evident in each Rossby and Froude number combination. These differences can be seen in Figure 11 (f = 0 s^{-1}) and Figure 12 (f = 1 x 10^{-4} s^{-1}). Figure 11 shows the presence of both cyclonic and anticyclonic rotation at a time of 66.67 hours and f = 0 s^{-1}, whereas Figure 12, at the same time but with f = 1 x 10^{-4} s^{-1}, shows predominately cyclonic rotation.

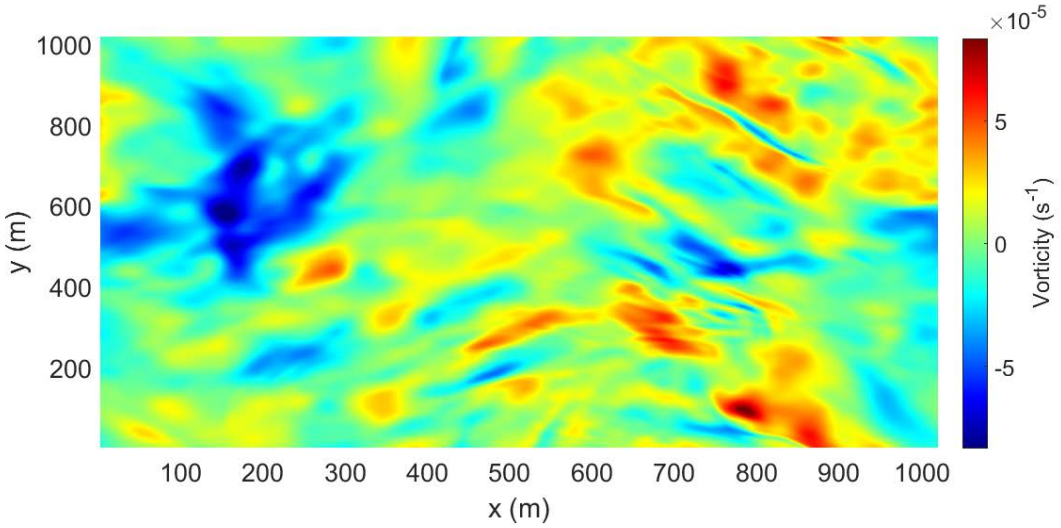

Figure 11. Vorticity cross section, f = 0 s^{-1}, U = 0.5 m/s, Fr = 15

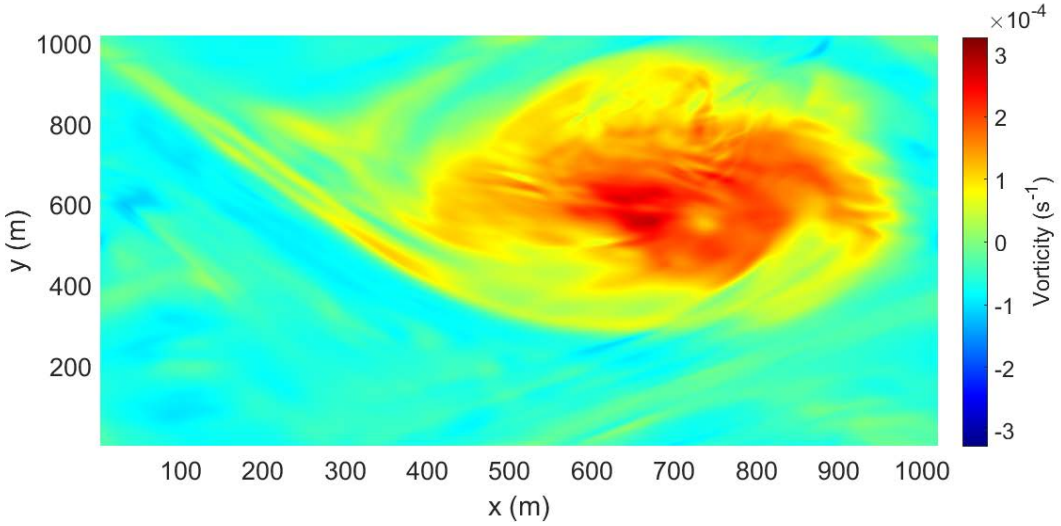

Figure 12. Vorticity cross section, f = 1 x 10^{-4} s^{-1}, Ro = 200, Fr = 15

In order to quantify these results, the MOW ratio *A* (Equation 9) introduced in Chapter II, Section C, was calculated at the end of each model run at time 66.67 hours. The results of all 24 model runs are shown in Tables 3 and 4.

Table 3. MOW value at t = 2.4 x 10^5 s (66.67 hours) with Coriolis

With Coriolis (f = 1 x 10^{-4} s^{-1})			
	Fr = 5	Fr = 15	Fr = 50
Ro = 20 U = 0.05 m/s	*A* = 0.49	*A*= 0.61	*A* = 0.67
Ro = 50 U = 0.125 m/s	*A* = 0.10	*A* = 0.80	*A* = 0.88
Ro = 200 U= 0.5 m/s	*A* = 0.67	*A* = 0.69	*A* = 0.82
Ro = 400 U = 1.0 m/s	*A* = 0.85	*A* = 0.75	*A* = 0.79

Table 4. MOW value at t = 2.4 x 10^5 s (66.67 hours) without Coriolis

Without Coriolis (f = 0 s^{-1})			
	Fr = 5	Fr = 15	Fr = 50
U = 0.05 m/s	A = -0.02	A = 0.05	A = 0.36
U = 0.125 m/s	A = 0.25	A = -0.37	A = 0.12
U= 0.5 m/s	A = 0.24	A = -0.14	A = 0.04
U = 1.0 m/s	A = -0.61	A = -0.16	A = 0.09

The results of the model runs conducted with the Coriolis force (Table 3) are characterized by positive *A*, reflecting cyclonic domination after 66 hours. In contrast, the results of the model runs without the Coriolis force (Table 4) are both positive and negative. Seven runs resulted in cyclonic dominated fields and five resulted in anticyclonic dominated fields. Of these, four runs were ±0.1 or less, reflecting a parity of cyclonic and anticyclonic rotation. The results found from the runs conducted with Coriolis are contrary to current thinking that pancake vortices are not affected by the rotation of the earth.

In addition to the 24 production runs, additional model runs were conducted with greater jet velocities. In one such run where U = 2.0 m/s, a unique difference was observed between the simulations with and without the Coriolis force. While examining the evolution of tracer patterns, a distinct crescent shape in the vertical axis developed with rotation run that was not seen in the without rotation run. Figure 13 shows this "Coriolis Crescent" at time 26.67 hours which is not visible in Figure 14, also at time 26.67 hours but without rotation.

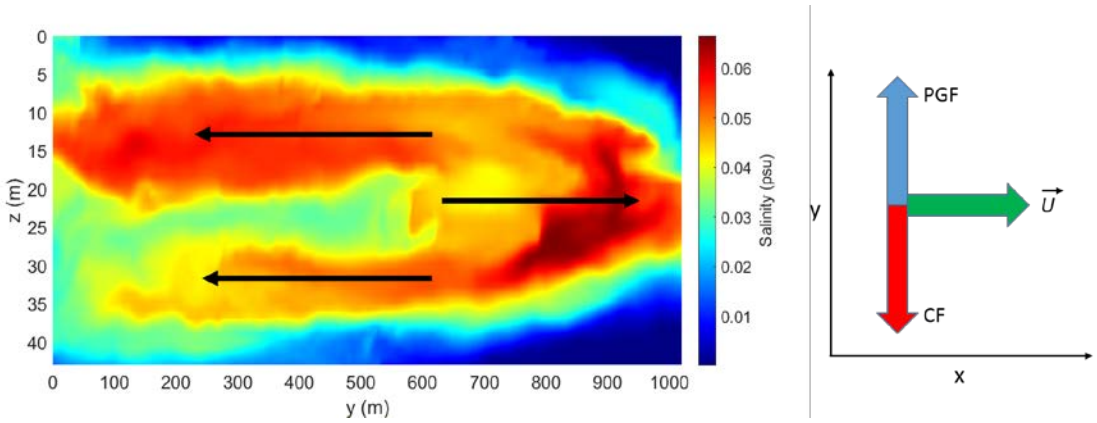

Figure 13. Tracer cross section, f = 1 x 10^{-4} s^{-1} with Coriolis Crescent

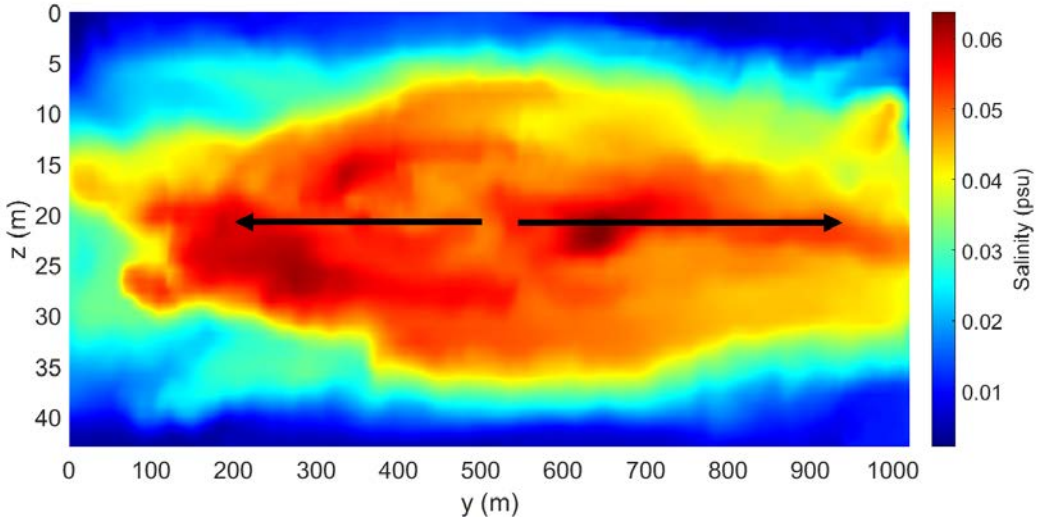

Figure 14. Tracer cross section, f = 0 s^{-1}

Without rotation, as in Figure 14, the jet-induced turbulence spreads symmetrically throughout the water column (as denoted by black arrows) whereas with rotation, as in Figure 13, turbulence spreads unevenly. A possible explanation for the Coriolis Crescent is a systematic failure of the initially imposed geostrophic balance of the pressure gradient force (PGF) and Coriolis force (CF). Without rotation, the force imbalance is not present and the spread of turbulence is unobstructed. However, with rotation, the flow dynamics becomes fundamentally different. As the jet decelerates in

time due to mixing of momentum, the Coriolis force rapidly weakens. The pressure gradient force, however, is controlled by the density distribution, and therefore its adjustment is less rapid than the change in the Coriolis force. As a result, the pressure gradient force dominates the Coriolis force in the latter stages of the experiment, resulting in the gradual displacement of fluid in the direction of PGF (Figure 13). Due to the incompressibility of sea water, this displacement of fluid in the positive y-direction at the level of the jet is accompanied by the corresponding drift of fluid in the opposite direction above and below the jet. The Coriolis Crescent effect may offer an in-situ method of target detection and tracking. By identifying the different aspects of the structure in the medium, a submarine or UUV may be able to better identify a submerged object's direction of movement.

THIS PAGE INTENTIONALLY LEFT BLANK

IV. DISCUSSION

A. CONCLUSIONS

The major finding of this study is that the earth's rotation does affect the vortices found in the late submarine wake. It has been shown through the use of otherwise identical model runs, with and without rotation, that distinct differences in the vortices develop over time. The largest distinction between them is the dissipation of anticyclonic vortices in the model runs that included rotation. This has been shown by inspection of the vorticity fields in the late stages of numerical experiments and quantitatively demonstrated by using MOW. In all 12 model runs with rotation, the integral MOW ratio (A) values were positive, as opposed to a mix of both positive and negative values in the runs without rotation. These positive values represent flow fields in which cyclonic rotation is greater than and persists longer than anticyclonic vortices. This contradicts and dispels the previously held assumption that both cyclonic and anticyclonic vortices persist in the late wake over time and dissipate at the same rate. Results also showed that high Rossby number simulations were affected by rotation, which is also contrary to current thinking. Results indicated that Rossby numbers as great as 400 are influenced by rotation. This revelation opens an entirely new line of inquiry into the dynamics of the late wake.

In addition to determining that the earth's rotation does affect late wake vortices, a new diagnostic parameter was introduced. After determining the presence of vortices via utilization of the Okubo-Weiss parameter, the direction and magnitude of rotation of vortices were calculated via the modified Okubo-Weiss parameter. Further research into pancake vortices will benefit from this ability to quantify the direction and magnitude of rotation.

B. OPERATIONAL RELEVANCE

In addition to affecting the oceanographic community, these results also have naval impacts. In an age where submarines have become increasingly quieter and thus increasingly difficult to detect acoustically, the utilization of hydrodynamic-based

detection and tracking methods is of the utmost importance. After identifying pancake vortices, it may be possible to more accurately locate and track submerged objects based on the current structure and rotational direction of the vortices. Unlike a submarine's acoustic signature, which must be detected when it is generated, the wake cannot be masked and remains evident to be detected for numerous days.

C. FUTURE RESEARCH

There are numerous opportunities for future research in this field. Further numerical modelling can be performed with more realistic parameters; in particular, an actual bluff-body wake would make for a more accurate starting condition than the simplified initial jet in this work. Given time and computing restraints, the model runs presented here are based on an initial perturbation caused by a jet. Continuing these model runs and utilizing a shape more representative of a submarine will help better tailor the results to the real-world environment. Longer duration model runs that provide results in excess of 65 hours would also be beneficial. Pancake vortices identified by satellites have been tracked for more than 10 days. Longer model runs would allow researchers to determine the full lifespan of pancake vortices and provide an estimate as to how long they can be tracked in the real world.

LIST OF REFERENCES

Beckers, M., R. Verzicco, H. Clercx, and G. Van Heijst, 2001: Dynamics of pancake-like vortices in a stratified fluid: Experiments, model and numerical simulations. *Journal of Fluid Mechanics,* **433**, 1–27.

Lin, J. T., Y. H. Pao, 1979: Wakes in stratified fluids: A review. *Annual Review of Fluid Mechanics,* **11**, 317–338, DOI:10.1146/annurev.fl.11.010179.001533.

Marshall, J., C. Hill, L. Perelman, and A. Adcroft, 1997: Hydrostatic, quasi-hydrostatic, and nonhydrostatic ocean modeling. *Journal of Geophysical Research: Oceans,* **102**, 5733–5752; DOI:10.1029/96JC02776.

Meunier, P., and G. R. Spedding, 2004: A loss of memory in stratified momentum wakes. *Physics of Fluids*, **16**, 298–305; DOI: 10.1063/1.1630053.

Moody, Z. E., C. J. Merriam, T. Radko, and J. Joseph, 2017: On the structure and dynamics of stratified wakes generated by submerged propagating objects. *Journal of Operational Oceanography*, **10**, 191–204.

Radko, T., 2001: Ship waves in a stratified fluid. *Journal of Ship Research*, **45**, 1–12.

Riley, J. J., and M. Lelong, 2000: Fluid Motions in the Presence of Strong Stable Stratification. *Annual Review of Fluid Mechanics*, **32**, 613–657; DOI: 10.1146/ 32.1.613.

Schooley, A. H., and R. W. Stewart, 1963: Experiments with a self-propelled body submerged in a fluid with a vertical density gradient. *Journal of Fluid Mechanics,* **15**, 83–96, DOI:10.1017/S0022112063000070.

Spedding, G. R., 1997: The evolution of initially turbulent bluff-body wakes at high internal Froude number. *Journal of Fluid Mechanics,* **337**, 283–301, DOI:10.1017/S0022112096004557.

Spedding, G. R., 2014: Wake signature detection. *Annual Review of Fluid Mechanics*, **46**, 273–302.

Sutyrin, G. G., and T. Radko, 2017: The fate of pancake vortices. *Physics of Fluids,* **29**, DOI: 10.1063/1.4977975.

van de Watering, Walter P. M., M. P. Tulin, and J. Wu, 1969: Experiments on turbulent wakes in a stable density-stratified environment. *Hydronautics, Incorporated*, 1–35.

Vortmeyer-Kley, R., U. Gräwe, and U. Feudel, 2016: Detecting and tracking eddies in oceanic flow fields: A Lagrangian descriptor based on the modulus of vorticity. *Nonlinear Processes in Geophysics,* **23**, 159–173, DOI:10.5194/npg-23-159-2016.

INITIAL DISTRIBUTION LIST

1. Defense Technical Information Center
   Ft. Belvoir, Virginia

2. Dudley Knox Library
   Naval Postgraduate School
   Monterey, California